THE PENNSYLVANIA STATE UNIVERSITY
SCHREYER HONORS COLLEGE

DEPARTMENT OF CHEMICAL ENGINEERING

DETERMINATION OF MICELLE SIZE THOUGH MICELLE FORMATION ENERGIES

TIMOTHY H. DIPAOLO
SPRING 2015

A thesis
submitted in partial fulfillment
of the requirements
for a baccalaureate degree
in Chemical Engineering
with honors in Chemical Engineering

Reviewed and approved* by the following:

Scott T. Milner
Joyce Chair and Professor of Chemical Engineering
Thesis Supervisor

Ali Borhan
Professor of Chemical Engineering
Honors Adviser

*Signatures are on file in the Schreyer Honors College.

Abstract

Surfactants form micelles when the concentration rises above the critical micelle concentration (CMC). The micelles have an optimal aggregation number, but the challenging equilibration hinders simulation measurements. For a surfactant solution to reach equilibration, the surfactants form micelles, the micelles reach conformational equilibrium, and multiple micelles share surfactants freely. While previous simulation has monitored micelle formation and conformational equilibrium, multiple micelles composed of sodium dodecyl sulfate (SDS) that freely share surfactants have not been observed. The time for full equilibration of SDS micelles far surpasses current computational capabilities. Previous research has used both coarse-grained and atomistic simulations to monitor the first two steps in the approach toward equilibrium. Once reached, the micelle equilibrium describes the optimal size of SDS micelles and the CMC, which prove valuable in many commercial and biological processes.

Rather than monitoring that free surfactants reach equilibrium in various micelles, we used simulation to find the free energy to remove a surfactant. By calculating and using the free energy of micelle formation, we estimated the optimal micelle size without equilibrating multiple micelles at a large time scale. Micelles ranging in size from 10 to 90 surfactants reached conformational equilibrium, which was confirmed by constant atom positions over time, diffusion of surfactants, and the spherical structure of the micelles. After reaching conformational equilibrium, the free energy for pulling a surfactant out of the micelle was calculated through umbrella sampling. Through the free energy for each size, the micelle formation energies were calculated. The optimal aggregation number was determined to be 75, with a polydispersity of $\pm$ 4 surfactants.

Table of Contents

List of Figures

List of Tables

Acknowledgements

I thank Dr. Scott Milner for stimulating my interest in chemical engineering and guiding me through this research the past two years. His vast knowledge helped lead the research to interesting conclusions. I am very thankful for the great opportunity I had as an undergraduate working in his research lab.

I thank Zifeng Li for helping me learn the programs, debug formulas and decipher data. Her aid provided understanding from small details to the large ideas about micelles. I also thank Dr. Darrell Velegol for providing an understanding of the experimental methods associated with micelles and for aiding the editing process.

I thank my parents for their constant encouragement. Whether traveling hours to track meets or just giving advice, they have always been supportive. Without them, I doubt I would be the person I am today.

Chapter 1

Introduction

Surfactants play an important role in many commercial and biological processes. The surfactant molecules contain a polar, 'hydrophilic' head group and a nonpolar, 'hydrophobic' tail. In solution, surfactants form micelles or bilayers when the concentration of molecules is higher than the critical micelle concentration (CMC). The head groups interact with the solution while the tails remain in the center of the micelle or layer.

Micelles allow compounds not soluble in polar solutions to solubilize. A few specific industry applications include aiding drug delivery studies, [1] solubilizing additives in foods, [2] and playing roles in textile manufacturing. [3] A common surfactant used in many processes is sodium dodecyl sulfate (SDS).

Figure 1.1 shows the structure of SDS and a cross section of a micelle composed of SDS. Simulation of micelles can provide further insight into micellular processes at the molecular level.

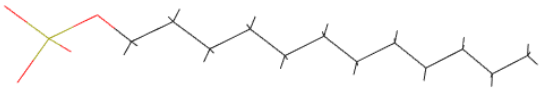

(a) SDS molecular structure.

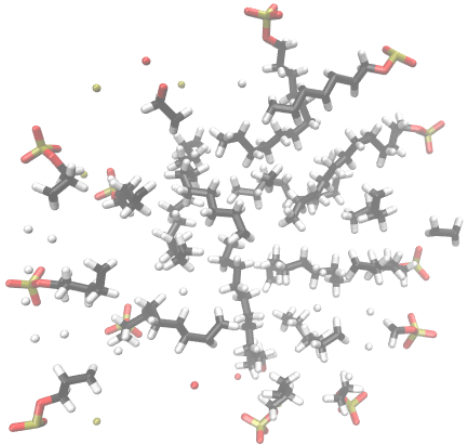

(b) SDS micelle.

Figure 1.1: SDS molecular structure and micelle cross section. of our simulated micelle of 60 surfactants. Red, yellow, black and grey represent oxygen, sulfur, carbon and hydrogen, respectively.

Many properties of a micelle can be experimentally observed, including the CMC, micelle size,

polydispersity, and surfactant exchange rate. By plotting surface tension and electrical conductivity versus the concentration of surfactants, the break in slope identifies the CMC. [4] Static (SLS) and dynamic (DLS) light scattering are used to find the micelle size. The time averaged intensity of light through the sample determines the micelle size in SLS. In DLS, the size is determined though the autocorrelation of the decay of the light. [5] Micelle polydispersity can be determined from dynamic light scattering through multiple autocorrelation functions. The rate of surfactant exchange can be measured through pulse radiolysis, where the exchange is measured between radioactively tagged and untagged micelles. [6].

Molecules can be simulated through either atomistic or coarse-grained models to analyze micelles. Atomistic models simulate each atom, while coarse-grained models represent portions of the molecule comprising multiple atoms as a single entity. While more accurate, atomistic simulations require more computer power.

There are multiple stages of equilibrium, including conformational equilibrium of a single micelle and equilibrium of a solution with multiple micelles. A single micelle can reach conformational equilibrium quickly, in which the structure of the micelle is stable. However, equilibrium of a surfactant solution arises when surfactants are shared freely between different micelles. For equilibration, the required simulation time far surpasses the capabilities of present day atomistic simulations.

Atomistic simulations to date have focused on conformational equilibrium of a single micelle, or on the process of initial assembly of micelles from dispersed surfactants. The structure of a micelle of 60 SDS molecules was analyzed by Bruce using atomistic simulations. [7] The equilibration time was recorded as 1 ns, and the simulations only lasted 5 ns. A single micelle was constructed and simulated in the simulation environment and no other sizes were analyzed. Equilibrium may not have been reached in the short simulation time.

Sammalkorpi allowed a 1 M, 700 mM, and 200 mM solutions of SDS molecules to equilibrate over 200 ns through atomistic simulation. The molecules were initially placed in random locations and self assembled into micelles. [1] During the simulation, around four micelles developed and

varied in size from 50 - 70 SDS molecules at room temperatures. However, the system did not fully reach equilibrium: the micelle sizes were still evolving at the end of the simulation. Sammalkorpi describes the results as analyzing the approach toward equilibrium. The lowest concentration (200 mM) remained well above the CMC, but further increases in system size were too computationally intensive.

Another atomistic simulation study on self-assembly was performed by Storm. [2] Similar results were obtained: long simulation times for self assembly of SDS micelles without fully reaching equilibrium.

Tang compared force field parameters for both coarse-grained and atomistic simulations. [8] Micelles of 60, 100, 300, and 382 SDS molecules were preassembled and simulated. For the smaller size micelles, the changes in force parameters had little effect and and remained largely spherical. Bicelles - mixtures between a micelle and bilayer - began to form in micelles of 300 or more aggregates. As the micelles were prefabricated, micelle equilibrium may not have been achieved.

Shang used coarse-grained modeling to create a large system of SDS. [9] The simplification of the atoms enabled simulation of the large system. SDS micelles were assembled and analyzed. The reported equilibration time was 1 ns, but surfactants were not freely shared between different micelles. Thus, the micelle may not have reached equilibrium in the simulation time.

LeBard used a coarse-grained model to monitor the self-assembly of surfactants to predict equilibrium states. [3] Multiple concentrations of SDS were analyzed for time periods ranging from 1.30 to 6.04 μs. The use of a coarse-grained model enabled long simulation times of large systems. Two stages of equilibration were found: the initial aggregation, which occurred in 50-400 ns, and the equilibration of micelle size distribution, which required simulation time too long to be performed. To reach full equilibrium even in the coarse-grained models, extremely long equilibration times may be required.

While previous simulations used both atomistic and coarse-grained simulation to analyze the the formation of micelles from free surfactants and the conformational equilibrium of micelles,

multiple micelles that freely shared surfactants were not observed. Bruce used atomistic simulation to view the structure of a conformationally equilibrated micelle. Sammalkorpi and Storm simulated free surfactants to monitor micelle formation with atomistic simulation. Tang monitored the conformational equilibrium of micelles for both atomistic and coarse-graned simulations. Shang and LeBard used coarse-grained simulation to analyze the conformational equilibrium and micelle formation, respectively. Full equilibration of micelle solutions in atomistic simulations, where multiple micelles freely share surfactants, remains beyond the scope of current computations.

However, there is another approach to determine the optimum micelle size from simulations, by focusing on the free energy to add or remove a single surfactant from micelles of various sizes. By computing the energy to add or remove a single surfactant from a micelle, the formation energy of a micelle can be calculated as a function of the micelle size. The formation energy is the sum of adding single surfactants to a micelle. The optimal micelle size occurs when the SDS micelle is in equilibrium with the SDS in solution. The size at the intersection of the micelle formation energy and free surfactant energy represents the optimal micelle size. Thus, the optimal size of a SDS micelle may be determined though the formation energy of the micelle.

Through atomistic simulation, a micelle composed of SDS can be established, simulated, and the properties predicted. By creating micelles of various sizes, the formation energy to add or remove surfactants can be calculated. The energy relies on the potential of mean force to pull a surfactant from the micelle. Umbrella sampling of the system determines the potential of the mean force. From the work to remove the surfactant, the formation free energy of the micelle can be calculated and used to compute the equilibrium micelle sizes. As each micelle can be equilibrated separately, the micelles do not need to reach an equilibrium state where the surfactants exchange freely between micelles. By imposing equilibrium between free surfactants and micelles in conformational equilibrium, the optimal size can be calculated. This greatly reduces the equilibration time to find the optimal size from the self-assembly models and simulations of multiple micelles in equilibrium.

Chapter 2

Methods

2.1 Overview

In the present work, individual preassembled micelles were equilibrated and simulated using atomistic simulations with explicit water. The use of CHARMM General Force Field [10] provided preexisting, accurate parameters for SDS molecules. TIP3P water surrounded the micelles as the CHARMM parameters were derived using TIP3P water. [10] Unlike other force field parameters, CHARMM accurately depicts micelles in high surfactant concentration. [8]

Since the approximate optimal micelle size is around 60 SDS molecules, the initial micelle contained 60 molecules. Later micelles varied from 10 to 90 molecules. With micelles containing fewer than 100 surfactants in this study, CHARMM continues to perform similar to other force fields at these micelle sizes and the micelle shape remains largely spherical. [8]

For each micelle size, an initial state of the molecules was created and simulated to equilibrate the system. A sulfur head was pulled from the equilibrated micelle and umbrella sampling used to determine the required energy.

The simulations used a 2 fs time step. The LINCS bond constraint algorithm maintained bond lengths throughout simulation. [11] The cut off radius was 1.1 nm and the van der Waals switch occurred at 1.0 nm. Particle-mesh Ewald (PME) method calculated the electrostatic parameters. [12] The GROMACS package performed all simulations. [13] Each system contained around 31,000 atoms.

2.2 Initial Micelle Configuration

Initial configurations for micelle simulations must be constructed carefully. To avoid immediate breakup of the micelle, the initial configuration should keep the hydrophilic head groups on the surface and the hydrophobic tails inside of the construction without overlap. For our simulations, we constructed a cube-shaped micelle, with the surfactant head groups on the surface of the cube, and the alkane tails in all-trans configurations directed into the cube along the x, y, and z axes,

shown in Figure 2.1. The cube contained the sulfur heads on the surface and the carbon chains on the inside. The coordinates of a single molecule was manipulated through translation and rotation to form the cube. The direction of the chains varied to maximize the number of sulfur heads on the exterior of the cube. When minimized, this allows the heads to interact with the water and counter ions and keep the hydrophobic tails on the interior of the micelle.

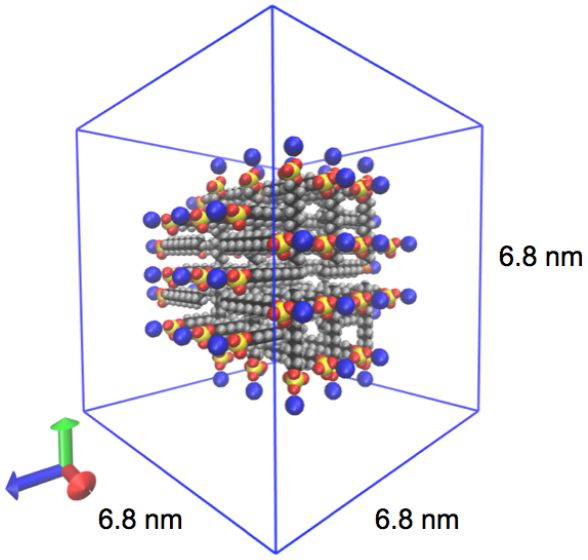

Figure 2.1: Initial configuration of SDS molecules in 6.8 nm cubic boundary.

Due to potentially large Coulomb forces, counter ions were placed close to each SDS head group to prevent dispersion of the surfactants. A sodium counter ion was placed 4 Å from the sulfur head along the backbone of the SDS molecule (Fig. 2.1). The close proximity enabled the ions to interact with the micelle during energy minimization simulations.

The molecules were placed in a simulation box with sides of 6.8 nm. Assuming an approximate micelle radius of 2 nm, the water - added after energy minimization - provides about a 1.4 nm buffer between the micelle and the boundary. A periodic boundary condition was placed in all directions to prevent issues with boundary effects. The large water buffer reduces interaction between the micelles across the boundary.

2.3 Equilibration

To prepare for a simulation, energy minimization reduced the magnitudes of the forces acting on the atoms in the initial cubic structure. Our cube-shaped initial micelle configuration was transformed to a more realistic spherical shape during energy minimization of the micelle. The steepest descent was used to quickly minimize the system to a lower energy state, and the L-BFGS algorithm [14] was used to find a more accurate lowest energy state. The energy was minimized both before and after the addition of water to reduce the water inside the micelle. Water inside the micelles lead to unfavorable interactions with the hydrophobic tail, which could cause the system to explode. In micelles with 80 or more surfactants, the energy of the micelle was minimized twice without water with a restrained counter charge simulation in between. This allowed the molecules to move and further be minimized without the counter charges migrating away. Otherwise, the micelles continued to break apart with the addition of water to the system. The energy minimization caused the micelle to condense, but did not form the spherical structure.

Once the energy was minimized, the temperature and pressure of the system were equilibrated. NVT (constant Number of atoms, Volume and Temperature) regulated the temperature of the system, while NPT (constant Number of atoms, Pressure and Temperature) equilibrated the pressure of the system. NVT simulation brings the system to the correct temperature. Differences in temperature within the system can cause artifacts during simulations. Velocity rescaling thermostat [15] enabled correct kinetic energy calculations, first order decay of temperature, and minimal oscillations. The 0.5 ns simulation brought the temperature to 360 K. The high temperature accelerated the equilibration of the micelle.

NPT simulation was performed in two phases: a Berendsen simulation [16] and a Parrinello-Rahman [17] simulation, both at 1 bar. The short 1 ns Berendsen simulation efficiently scale the box before a run, but resulted in an incorrect thermodynamic ensemble. A 10 ns Parrinello-Rahman simulation corrected the thermodynamic ensemble. Only the Parrinello-Rahman data was used for the analysis.

Restraining the center of mass of the micelle reduced adverse interactions with the boundary conditions. Originally during the simulations, the micelle could move freely within the boundaries. However, if the micelle hit the periodic boundary conditions, the center of mass would reflect the center of mass of the molecules in the simulation box rather than the center of mass of the micelle. As some of the molecules appeared on the opposite size of the box, the center of mass moved toward the center of the box. The distance between the pulled sulfur atom and the center of mass of the micelle then became incorrect. Thus, a harmonic potential was placed on the center of mass of the sulfur heads of the micelle to restrain the micelle to the center of the box during equilibration with a spring constant of 1,000 kJ mol^{-1} nm^{-1}. With the center of mass was restrained, the individual surfactants could both diffuse across the micelle and move into or out of the micelle as needed, as long as the actions of the molecules were balanced. The equilibration of temperature and pressure created the spherical micelle structure.

2.4 Initial Configurations for Umbrella Sampling

To find the free energy to add or remove a single surfactant from a micelle, we determined the potential of mean force for pulling the surfactant head away from the micelle center. The potential of mean force is obtained from a series of simulations in which a single surfactant is restrained in three dimensions by an umbrella potential to reside near a certain distance from the micelle center. This allowed access to regions that would be difficult analyze, due to the interactions pulling the surfactant back into the micelle. The hydrophobic interactions create a favored sulfur distance from the center of mass, resulting in a minimum in energy at the distance.

For each micelle size, the calculation of the energy changes of the micelle required the acquisition a maximum and minimum in energy, shown in Figure 2.2. The difference between the maximum and minimum in energy is the binding energy. Without a clear maximum and minimum, the binding energy may not be the full energy to remove a surfactant. For example, if the surfactant was already partially free of the micelle, the energy difference between the initial and final states

would only be a portion of the energy required to pull a surfactant from the micelle. For uniform energy measurements across the various micelle sizes, the minimum and maximum energies were obtained.

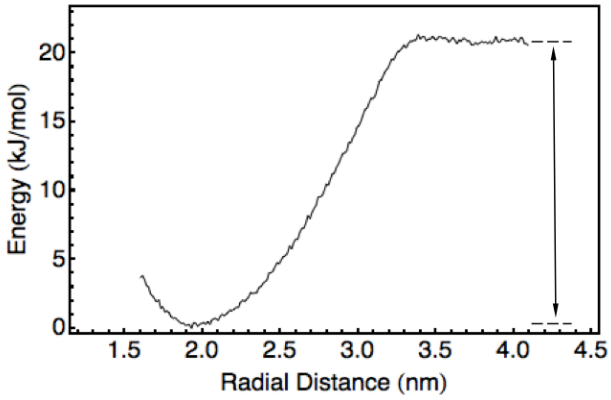

Figure 2.2: Example of a PMF graph. The arrow represents binding energy.

To ensure the sulfur head reached the minimum during the pulling, the molecule was pushed into the micelle, resulting in a higher energy state due to more interactions with the hydrocarbons. The pushing and pulling occurred along the vector from the molecule's sulfur head to the center of mass of the micelle. The push phase lasted 100 to 300 ps depending on the micelle size and the pull phase lasted up to 2 ns. Both simulations used a spring constant of 4,000 kJ mol^{-1} nm^{-1}, a pull rate of 0.0020 nm/ps, and occurred at 310 K. The pull rate enabled the molecule to become completely free of the micelle during the simulation.

2.5 Umbrella Sampling

Umbrella sampling analyzes the energy of the system through a series of frames: the energy of each frame combines to form an energy profile. A harmonic umbrella potential was placed on the sulfur and the micelle center of mass. The pull rate of 0 nm/ps kept the distance in each frame about constant throughout the analysis. The selected frames were every 0.15 nm along the radial trajectory. Each umbrella sample ran for 10 ns with a spring constant of 1,000 kJ mol^{-1} nm^{-1}. The spring constant was compared to trials with constants of 250 mol^{-1} nm^{-1} and 4,000 kJ mol^{-1}

nm^{-1}. 1,000 mol^{-1} nm^{-1} resulted optimized the number of samples and resulted in low errors.

The various histograms of head groups versus radial distance were combined to form the energy profiles using weighted histogram analysis method (WHAM). WHAM uses bootstrap analysis to calculated the energy profiles, or potential of mean force (PMFs). [18] The bootstrap method calculated new trajectories based on the umbrella histograms. The energy profile shows the energy change as the molecule is pulled from the micelle. Several molecules were pulled out of the micelle in different pulling simulations. The samples for the molecules were combined to average the energy profiles.

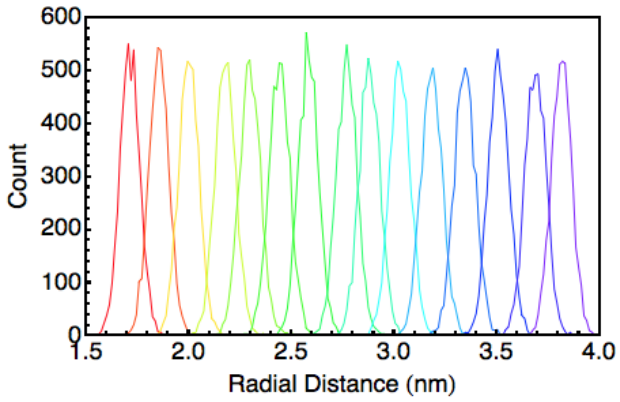

Figure 2.3: Example histograms from PMF graph. Proper spacing of histograms is required for sufficient overlap.

Histograms showed the overlap between the samples used in the umbrella sampling; sufficient overlap was required to avoid discrepancies in the curve. Gaps between histograms resulted in large deviations from a smooth curve. Figure 2.3 shows the histogram created while calculating the potential of mean force graph. The histogram shows the distance of the molecule to the center of the mass for each frame used in the calculations. As the energy graphs do not have large disturbances of the curve, the frame spacing was sufficient.

Chapter 3

Results and Discussion

3.1 Overview

With the transformation of the cubic initial state to the spherical, micellular structure, the surfactants were conformationally equilibrated, which was verified by various measures before calculations of formation energy. The 10 ns of the second NPT simulation were used for the analysis of each micelle size. Figure 3.1 shows the spherical, equilibrated micelle. For equilibration of a single, prefabricated micelle, the atom position and spherical structure of the micelle should remain constant and the surfactants should diffuse throughout the micelle. Before the computation of the formation energy, we confirmed the equilibrium states of each size micelle.

With conformational equilibrium reached, the potential of mean force graphs were created for the calculation of the binding energy. The micelle formation energies were derived from the binding energies and, with the common tangent, used to calculated the optimal micelle aggregation size. Through equilibrium between the micelles and surfactants, the polydispersity was modeled and calculated. As counter ions were added to the system, we analyzed potential salt effects on the aggregation size.

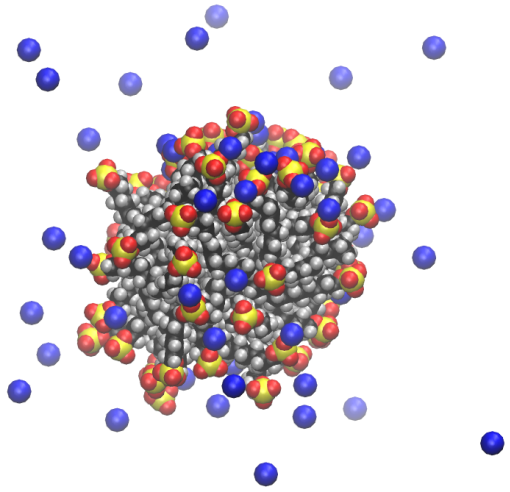

Figure 3.1: Spherical structure of equilibrated micelle of 60 SDS molecules.

3.2 Micelle Shape

For further insight into the structure, the average distance between each atom type and the center of the micelle was monitored. The average atom positions for the micelle containing 60 SDS molecules and the distribution of atom distance to the center of mass of the micelle are seen in Figure 3.2.

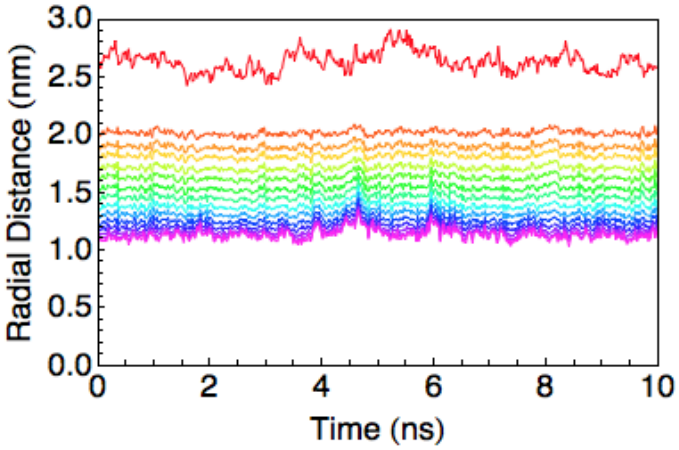

(a) Average position over time.

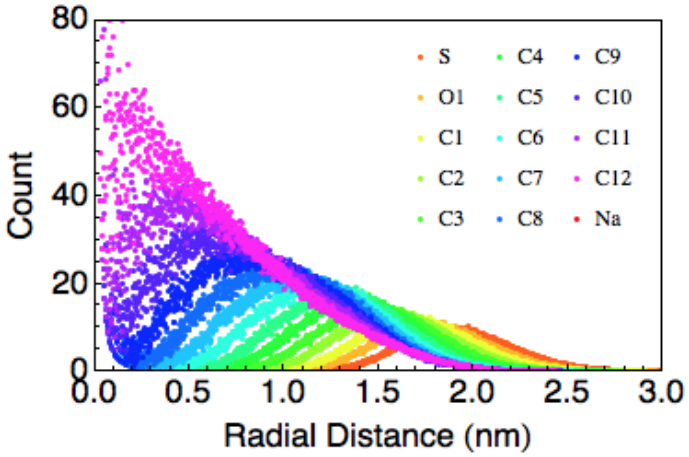

(b) Distributions of atom position for the 60 SDS micelle.

Figure 3.2: Constant average atom distances over time show equilibrium state of the micelle and distribution of atom location with respect to center of mass of the micelle.

Although the micelle is a perpetually changing spherical structure, the the time-independent average radial positions of each atom along the chain are an indication of conformational equilibrium.

The sulfur heads remained on the outer surface of the micelle, while the atoms in the hydrophobic tails retained their chain positions inside the micelle, shown in Figure 3.2(a). Bruce obtained similar values and trends while analyzing the structure of a prefabricated micelle of the same number of surfactants.[7]. As the size of the micelles increased, the radial distances increased, but the specific atom distance trends persisted for the each micelle size.

The distributions of atoms shows the distance from the center of mass of the micelle to each atom throughout the simulation, shown in Figure 3.2(b). The polar heads remain at the exterior of the micelle, and the end of the non polar tail lies closer to the center of mass, as shown by the averages, or peaks, of each radial distribution function. The spherical structure and the distances of the atoms provided preliminary confirmations of structure equilibrium.

3.3 Diffusion

During conformational equilibrium, the surfactants diffuse across the surface of the micelle, so we verified the diffusion of the sulfur heads through autocorrelation functions. Reasonable diffusion times confirm conformational equilibrium. The diffusion of the molecules was analyzed both visually and numerically.

The positions of nine sulfur heads were monitored throughout the entire 10 ns NPT simulation. In the initial configuration, the nine sulfur heads were initially on one side of the micelle cube. Over time, the sulfur heads diffused across the micelle surface and the time traces complete the spherical micelle structure, as seen in Figure 3.3(a). The other 51 SDS molecules diffused across the micelle surface in a similar fashion. Together, the surfactants diffused across the entire surface of the micelle, as desired in micelles in conformational equilibrium.

In addition to visually monitoring the movement of the molecules, autocorrelation functions were applied to the distance from each sulfur head to center of micelle over time. The autocorrelation function was calculated through the equation

$$C(t) \simeq \frac{1}{N-t} \sum_{i=1}^{N-t} d_{i+t} d_i \tag{3.1}$$

where N is the number of steps in the time series and d is the distance between sulfur head and center of mass of the micelle over time. The decay of the function over time describes the relationship between the sulfur atom positions.

The linear portion of a log plot of the autocorrelation function describes the time required for diffusion to occur. An exponential fit can be used to find the diffusion time through

$$C(t) = \alpha e^{\frac{-t}{\tau}} \tag{3.2}$$

where τ is the diffusion time and α is a constant. The autocorrelation function and the linear fit are shown in Figure 3.3

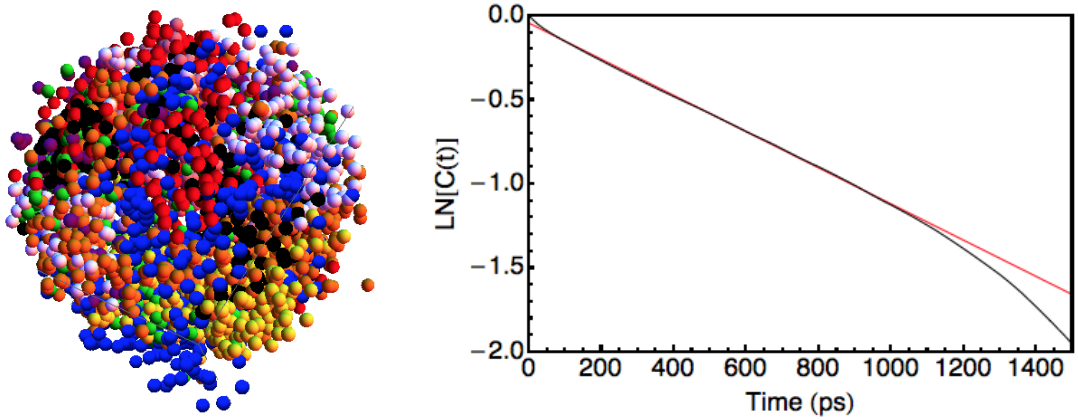

(a) Sulfur head diffusion.

(b) Diffusion Graph.

Figure 3.3: Visual representation of diffusion through nine selected sulfur head positions over 10 ns and autocorrelation function with linear fit of data for a micelle containing 60 SDS molecules.

For conformational equilibration to occur, the head groups require enough simulation time for diffusion across the micelle surface. The simulation time needs to be a few times longer than the diffusion time for proper diffusion. The diffusion time for each micelle size was less than the simulation time and is recorded in Table 3.1, seen at the end of the chapter. The NPT equilibration of each micelle was monitored and largest diffusion time was 0.97 ns, or less than a tenth of the

simulation time. While the smaller micelles had ample time to diffuse (up to about 27 times the diffusion time), longer equilibration times may provide the larger micelles with further diffusion.

3.4 Spherical Structure

As the size of the micelles grows with increasing number of surfactants, the shape can diverge from the spherical structure to a bilayer, so the shape of each micelle was monitored through the simulations. In a bilayer, the spherical structure flattens to form layers rather than a micelle. As the formation energy of a micelle differs from that of a bilayer, the maintenance of a spherical structure was required.

The average distance from the sulfur heads to the center of mass of the micelle is shown in Figure 3.4. As expected, the larger the number of SDS molecules in the micelle, the larger average sulfur distance to the center of mass. With more SDS in the micelle, the radius must expand to accommodate for hydrophilic interactions of the head groups and hydrophobic interactions of the tails.

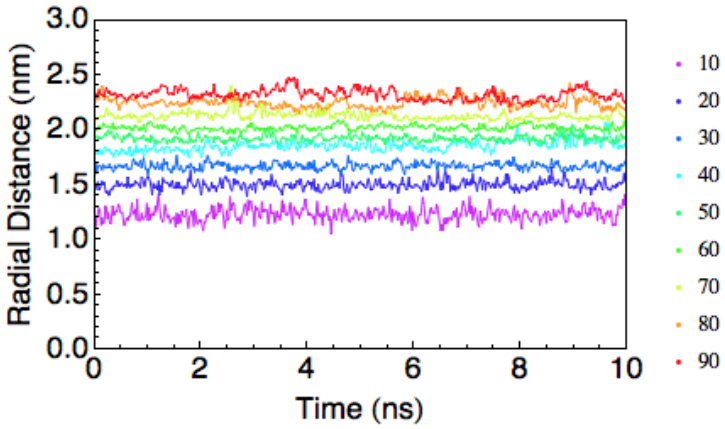

Figure 3.4: Average distance from sulfur heads to center of mass of the micelle throughout equilibration of micelle. Micelles range from the 10 SDS micelle in purple to the 90 SDS micelle in red.

Radial distribution of the sulfur head groups show the changes in radial size and shapes of the micelles. Figure 3.5 also contains the radial distribution function plots. The shifting of the radial

distribution function peaks show the increase in radial size. However, as the size increases, the width of the radial distribution widens and may reflect shape changes in the micelle. The large number of molecules fighting for interactions can cause the sphere to deform. Although the largest of the micelles may have slight deviations from the spherical structure, the equilibration of each micelle is shown though the the micelles remaining largely spherical and the constant average radial distance of the sulfur heads.

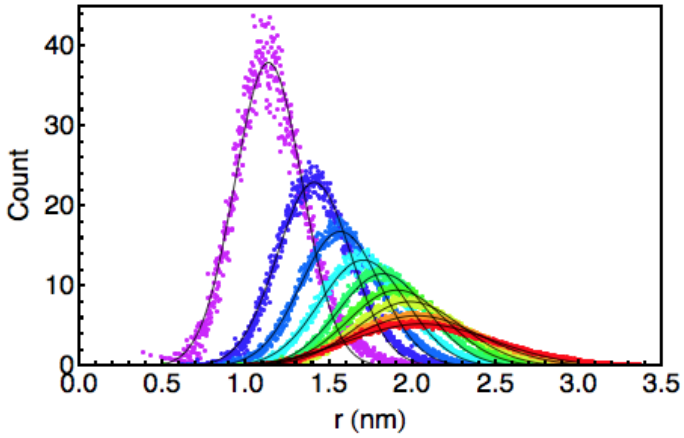

Figure 3.5: Radial distributions of the sulfur heads for each micelle size. Micelles range from the 10 SDS micelle in purple to the 90 SDS micelle in red.

As the radial distribution functions flattened as the micelle size increased, analysis of the radius and variance showed how large the deviations were for each micelle size. The radial distribution functions were fit with gaussian curves to determine the radius and variance. The gaussian fits were of the form

$$f(r) = aExp(\frac{-(r - r_o)^2}{2\sigma^2}) \tag{3.3}$$

where r_o is the average radius and σ^2 is the variance.

When plotted versus number of surfactants, the initial values for the radius cubed, r_o^3, deviated from linearity in the larger micelles, as shown in Figure 3.6(a).

The structure of the micelles containing more surfactants became less spherical. As the micelle size increase, the spherical structure may become distorted with valleys and peaks. While the

average sulfur radial distance continues to grow, the range of distances grows, as shown in Figure 3.6(b). The shell the sulfur atoms occupy around the micelle increases in thickness. The variance describes the size of the shell of sulfur heads. Thus, the variance, σ^2, used to account for the changes in r_o^3 values through

$$<\delta r_o^2> = \sigma_{app}^2 - \sigma_o^2 \tag{3.4}$$

$$r_o^{3'} = <r_o^3> + 4\pi <r_o><\delta r_o^2> \tag{3.5}$$

where σ_o^2 was established through the gaussian fit and σ_{app}^2 through a linear fit of the σ^2 values.

The plots of $r_o^{3'}$ and σ^2 versus the number of surfactants are seen in Figure 3.6. The original $r_o^{3'}$ values are presented with circles and the adjusted values with plus signs. The values of r_o and σ^2 for each micelle size are tabulated in Table 3.1 at the end of the chapter. When the variance is taken into account, the radial size of the micelle increases regularly with increases in number of SDS. The deviations from the trend confirm the micelles becoming less spherical, as shown by the radial distribution function graphs.

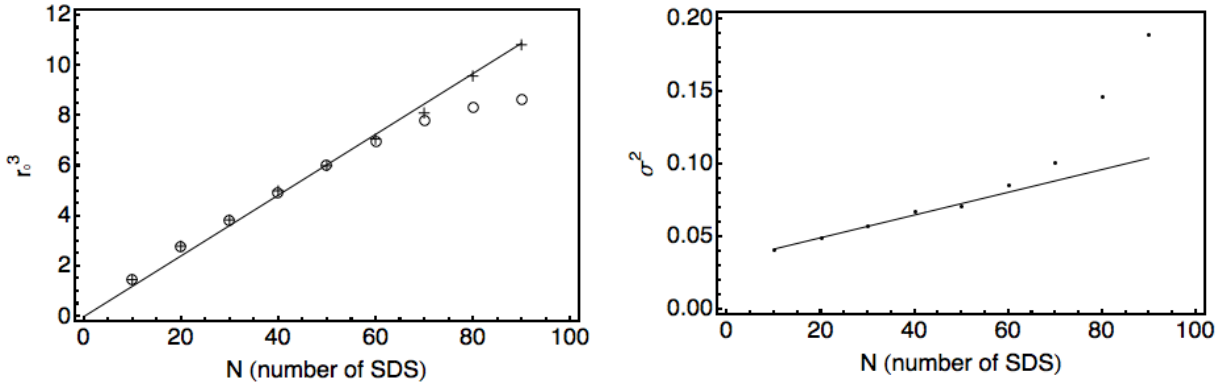

(a) Radius cubed graph.

(b) Variance graph.

Figure 3.6: Cubed average radial distance from the sulfur heads to the center of the micelle, $r_o^{3'}$. Circles represent original data while plus signs show effect of variance. Variance, σ^2, versus number of surfactants also shown.

Further increases in micelle size may cause more shape distortions. This would alter the overall micelle energy as the SDS molecules can interact with more molecules as the structure moves towards a bilayer. The interacts would alter the formation energy. The deviations from spherical

in the largest micelles may have a slight effect, but most of the micelles retained the equilibrated, spherical shape throughout simulation.

3.5 Potential of Mean Force

With the equilibrium of the micelles established, pulling the molecules out of the micelle enabled the calculation of the potential of mean force. The potential of mean force was plotted over the distance between the pulled sulfur atom and the center of mass to create energy profiles. The energy change enables the calculation of the free energy. Due to the push of the molecule into the center of the micelle, the energy reached a minimum at the optimal radial distance. Once the molecule was pulled away from the micelle, it reached a point where the micelle no longer had an effect on the energy of the molecule. The binding energy is the difference between the minimum and plateau (Fig. 2.2).

The energy profile for each micelle size is seen in Figure 3.7. Each energy profile has been shifted so that its minimum energy is zero. As expected from the sulfur distance and radial distribution plots, the minimum, or optimal location, increases in the micelles with more surfactants. The difference in energy is the energy barrier to remove a surfactant. After the initial barrier, often, the energy declines as the surfactant moves further from the micelle. This represents the binding energy and is the energy used in the formation energy calculations. Micelles with too few or too many surfactants have a lower barrier than the middle sizes, which are closest to the optimum size.

Interactions between the surfactants and the solvent have an impact on the energy barrier for micelles of different sizes. Micelles with few surfactants have a low energy difference that builds as the size increases. After a plateau, the energy difference decreases again. The energy difference is the cost to expose a hydrophobic tail. At low micelle sizes, the tails already have high interactions with the water, so removing a surfactant does not require significant work. In the large micelle sizes, the surfactants become crowded, and the increase in surface area is not well covered by the sulfur heads, allowing higher interaction between the chains and the water. While the large and

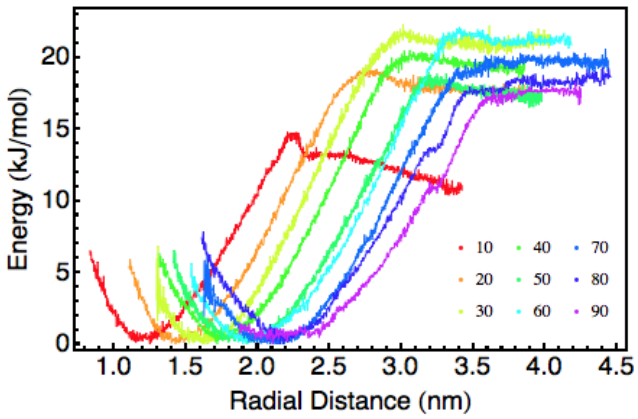

Figure 3.7: PMF graphs as SDS molecules is pulled from micelle. Micelle sizes ranged from 10 surfactants in red to 90 surfactants in purple.

small micelles shed surfactants easily, sizes closer to the optimal size have proper interactions to maintain surfactant levels.

The diffusion times were also calculated for the umbrella samples used to create the potential of mean force graphs. The autocorrelations were between the sulfur atom and the center of mass of the micelle. For the umbrella samples, the diffusion times were on the order of a few picoseconds. Figure 3.8 shows the autocorrelation times for the umbrella samplings used for the micelle containing 40 surfactants. The maximum was 59.0 ps. Thus, the umbrella runs of 10 ns provided a minimum of 169 times the autocorrelation time, or amble time to equilibrate for the energy profiles. The large increase in autocorrelation time at 3 nm reflects the point where the chain just breaks free of the micelles. As the tail switches between interaction with the micelle and breaking free, it requires more time for equilibration. Both during simulation before pulling the molecules and before umbrella sampling, the diffusion of the molecules show the micelles reaching an equilibrium state.

3.6 Free Energy

The potential of mean force graphs enable the calculation of the optimal micelle size. Integration of the binding energy enables the calculation of the free energies of the micelles. The energy

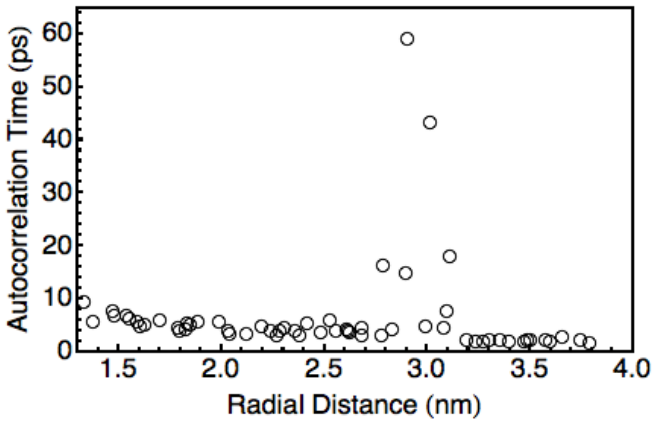

Figure 3.8: Autocorrelation times between sulfur atom and micelle for umbrella samplings performed for 40 SDS micelle.

depends on the energy to expose the carbon chain. The cost is less for the small and large micelles: the tail is largely exposed in the small micelles, and crowding enables spontaneous shedding of surfactants in large micelles. As the integration of the binding energy increases with micelle size, the rate of ascent decreases. For the micelle to be in equilibrium with the free surfactants, the energy of free surfactants must be equal to that of the surfactants in the micelle. Thus, a common tangent can be drawn from the origin to a point of tangency on the integrated energy curve. The point of tangency represents the optimal micelle size and CMC.

Calculation of the energy integration graph relied on the energy differences from the PMF curves. The differences in energy for each micelle size is recorded in Table 3.1 and plotted in Figure 3.9. A line representing the energy of the free surfactants was subtracted from the integration of the PMF curves. The average between binding energy points was used to create the integration of the energy curve though point integration. The point of tangency occurs at 75 surfactants, where the difference between the free surfactant energy and the micelle formation energy is zero. Figure 3.9(b) shows the difference between the two energies.

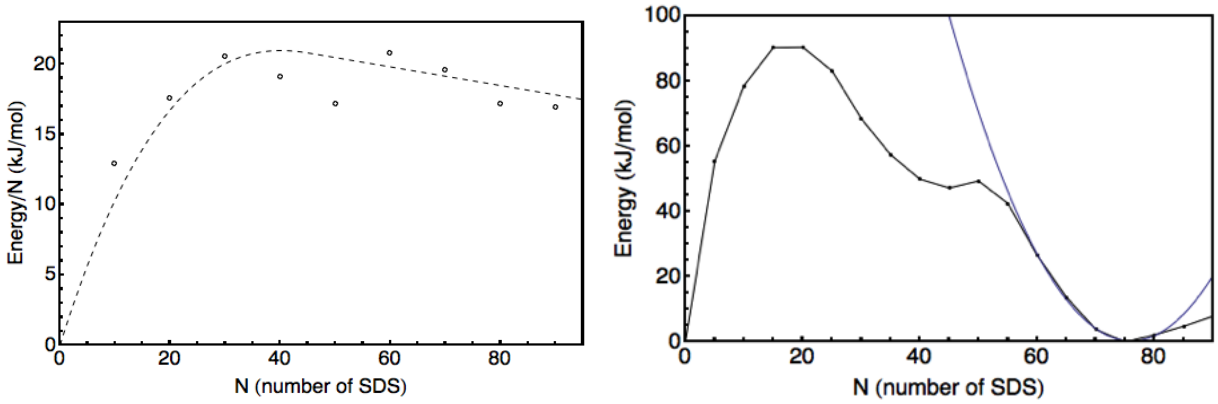

(a) Energy Graph.

(b) Difference between Energy Graph Integral and Tangent Line.

Figure 3.9: Energy differences on PMF graphs versus number of surfactants in micelle. Difference between integral of energy difference and free surfactant energy line. Blue polynomial fit describes polydispersity.

Table 3.1: Comparison of radius (r_o), variance, (σ^2), diffusion time (τ), and energy difference (E) for each micelle with N SDS molecules.

N	$r_o(m)$	σ^2	τ (ns)	$E(kJ/mol)$
10	1.13	0.041	0.37	12.9
20	1.41	0.049	0.38	17.5
30	1.57	0.057	0.62	20.5
40	1.71	0.068	0.62	19.1
50	1.82	0.071	0.75	17.1
60	1.92	0.086	0.93	20.7
70	2.01	0.101	0.89	19.5
80	2.12	0.146	0.89	17.1
90	2.21	0.189	0.97	16.9

3.7 Common Tangent

The equilibrium can be modeled as a mixture of ideal gases of micelles of different sizes. The free energy model accounts for the number of surfactants in micelles, the translational entropy of the micelles, and the translational entropy of the surfactants in the micelles. The free energy can be expressed though

$$F = \sum N_n/n(U_n + kT(log(c_n V_0) - 1) + (n-1)kTlog(c_h V_0)) \tag{3.6}$$

Where N_n is the number of surfactants in the micelles of size n, c_h is the ideal gas concentration of surfactant in the corona, $c_n V_0$ is the volume per surfactant in the corona, and c_n is the concentration of micelles of size n.

$$0 = U_n - U_{n-1} + kTlog(c_n/c_{n-1}) - kTlog(c_1/c_h) \tag{3.7}$$

This represents the equilibrium condition for pulling out a single surfactant. Through minimization of the free energy with respect to the number of surfactants in micelles and imposing a Lagrange multiplier, an equilibrium condition between the micelle and surfactants was established. Again, the equilibrium depends on the equilibrium between the micelles and the free surfactants. Where the equilibrium of the micelle and free surfactants meet is the common tangent. As the free energy depends on the building from a free chain, micelles of sizes similar to the optimal size will also appear in the solution creating polydispersity.

3.8 Polydispersity

The polydispersity describes the varying sizes of micelle in equilibrium and can be determined from the free energy. The concentration of micelles near the optimal size, n^*, can be described by the equation

$$c_n/c_h = e^{-\beta(U_{n^*} + (1/2)U''_{n^*}(n-n^*)^2)} \tag{3.8}$$

where c_n is the concentration on n near n^*, c_h is the final concentration, and U_{n^*} is the energy. Derived from Legrange multipliers and equilibrium between the micelles and surfactants, Equation 3.8 describes the size distribution of the polydisperisty through

$$\Delta n^2 = 1/(\beta U''_{n^*}) \tag{3.9}$$

A parabolic fit of the difference between the formation energy and surfactant energy is seen in

Figure 3.9(b). Through temperature of the system, the Boltzmann constant, and the parabolic fit (U_{n^*}) in Equation 3.9, the size distribution of the system was 3.8. Thus, the polydispersity is 75 $\pm$ 4 surfactants.

3.9 Salt Effect

Salt in the system has an effect on the micelle size and CMC. While the system did not have any added salt, the sodium ions that were assembled with the micelle did not all interact with the micelle. Increases in salt concentration result in lower CMC and higher aggregation numbers, due to the ionic shielding. [5] Typical aggregate sizes at room temperature lie between 60 and 70 surfactants. [7] As aggregation size of 75 $\pm$ 4 surfactants lies above the typical size, the sodium ions in the solution may have increased the aggregation number. Assuming the ions in the solution were spread though out the water in the simulation, salt concentrations were calculated. The approximate salt concentration was 0.22 M of sodium. Experimental data shows an aggregation number of approximately 90 aggregates for 0.22 M salt solution. [19] As some of the simulated sodium ions interact with the micelle, the salt effect would result the aggregation number lower than 90 aggregates, as was achieved. With the rise in aggregate number from the salt concentration, the acquired aggregation size of 75 $\pm$ 4 is similar to experimentally derived values.

Chapter 4

Conclusion

Through the free energy of formation, we found the optimal micelle size without having to simulate multiple micelles. As current computational power cannot sustain simulation for lengths required for equilibrium, most previous work focuses on conformational equilibrium or self assembly of micelles. Without reaching equilibrium, estimations of the optimal size may be skewed.

In this research, micelles of sizes from 10 to 90 surfactants were simulated and brought to conformational equilibrium. The equilibrium state was shown through the constant average atom positions over time and the diffusion calculations. As the structure remained relatively constant and the atoms freely diffused across the surface, the micelle had reached conformational equilibrium.

In addition to atom position stability, the structure of the simulated micelles further was spherical. The radial distribution functions analysis showed spherical nature, with the slight deviations in the larger micelles.

By pulling a surfactant from the micelle, the energy to pull out a surfactant was determined for each size micelle and used to find the formation energy. The integration of energy for each micelle size enabled the calculation of free energy. Fully equilibrated micelles are also in equilibrium with the surfactants in the surrounding fluid. The common tangent intersected the energy integration graph tangentially at 75 surfactants. The aggregate size was determined to be 75 surfactants.

As the salt concentration may have been affected by excess sodium ions in the water, the aggregation size would increase. The elevated micelle size from the experimentally 60-70 surfactants at room temperature may be due to the salt effect. Polydispersity calculations from the free energy graph found the micelles to be 75 ± 4 surfactants. The use of free energy enabled the calculation of the aggregation size of micelles by using only enough simulation time to bring conformational equilibrium.

Calculation of the optimal micelle size without having to simulate multiple micelles provides several directions for further research. In this work, the salt concentration was due to ions that enabled micelle neutrality. Simulation of the micelles with high salt concentration could be compared to experimental measurements of micelle size. Through the comparison, the reliability of simulation predictions of the salt effect could be analyzed. The method could also be applied to

surfactants other than SDS for comparison to their experimental optimal aggregation size. Systematic trends may be expected as the chain size changes.

Bibliography

[1] M. Sammalkorpi; M. Karttunen; M. Haataja. Structural properties of ionic detergent aggregates: A large-scale molecular-dynamics study of sodium dodecyl sulfate. *J. Phys. Chem. B*, 111(40):11722–11733, 2007.

[2] S. Storm; S. Jakobtorweihen; I. Smirnova; A. Panagiotopoulos. Molecular dynamics simulation of sds and ctab micellization and prediction of partition equilibria with cosmomic. *Langmuir*, 37(29):11582–11592, 2013.

[3] D. LeBard; et. at. Self-assembly of coarse-grained ionic surfactants accelerated by graphics processing units. *Soft Matter*, 8:2385–2397, 2012.

[4] P. Mukerjee; K. J. Mysels. Critical micelle concentrations of aqueous surfactant systems. *NSRDS-NBS*, 1971.

[5] C. A. Gracia; S. Gomez-Barreiro; A. Gonzalez-Perez; J. Nimo; J. R. Rodriguez. Static and dynamic light-scattering studies on micellar solutions of alkyldimethylbenzylammonium chlorides. *Journal of Colloid and Interface Science*, 276:408–413, 2004.

[6] M. Almgren; F. Grieser; J. K. Thomas. Rate of exchange of surfactant monomer radicals and long chain alcohols between micelles and aqueous solutions. *Pulse Radiolysis of NaLS in Micelles*, pages 1674–1687, 1978.

[7] C. Bruce; M. Berkowitz; L. Perera; M. Forbes. Molecular dynamics simulation of sodium do-

decyl sulfate micelle in water: Micellar structural characteristics and counterion distribution. *J. Phys. Chem. B*, 106(15):3788–3793, 2002.

[8] X. Tang; P. Koenig; R. Larson. Molecular dynamics simulations of sodium dodecyl sulfate micelles in water - the effect of the force field. *J. Phys. Chem. B*, 118(14):3684–3880, 2014.

[9] B. Shang; Z. Wang; R. Larson. Molecular dynamics simulations of interactions between a sodium dodecyl sulfate micelle and a poly(ethylene oxide) polymer. *J. Phys. Chem. B*, 112(10):2888–2900, 2008.

[10] A. D. Mackerell; N. Banavali; N. Foloppe. Development and current status of the charmm force field for nucleic acids. *Biopolymers*, 56(4):257–265, 2000.

[11] B. Hess; H. Bekker; H. J. C. Berendesen; J. G. E. M. Fraaije. Lincs: A linear solver for molecular simulations. *Journal of Computational Chemistry*, 18(12):1463–1472, 1997.

[12] T. Darden; D. York; L. Pedersen. Particle mesh ewald: An $n \cdot log(n)$ method for ewald sums in large systems. *The Journal of Chemical Physics*, 98(12):10089–10092, 1993.

[13] H. J. C. Berendsen; D. van der Spoel; R. van Drunen. Gromacs: A message-passing parallel molecular dynamics implementation. *Computer Physics Communications*, 91(1-3):43–56, 1995.

[14] R. Byrd; P. Lu; J. Nocedal; C. Zhu. A limited memory algorithm for bound constrained optimization. *SIAM Journal on Scientific Computing*, 16(5):1190–1208, 1995.

[15] G. Bussi; D. Donadio; M. Parinello. Canonical sampling through velocity rescaling. *Journal of Chemical Physics*, 126(1), 2007.

[16] H. J. C. Berendsen ; J. P. M. Postma; W. F. van Gunsteren; A. DiNola; J. R. Haak. Molecular dynamics with coupling to an external bath. *The Journal of Chemical Physics*, 81(8):3684–3690, 1984.

[17] A. Parinello, M.; Rahman. Polymorphic transitions in single crystals: A new molecular dynamics method. *Journal of Applied Physics*, 52(12):7182–7190, 1981.

[18] J. S. Hub; B. L. de Groot; D. van der Spoel. g-wham - a free weighted histogram analysis implementation including robust error and autocorrelation estimates. *American Chemical Society*, 6(10):3713–3720, 2010.

[19] N. Mazer; G. Banedek; M. Carey. An investigation of the micellar phase of sodium dodecyl sulfate in aqueous sodium chloride solutions using quasielastic light scattering spectroscopy. *J. Phys. Chem.*, 80(10):1075–1085, 1976.

Timothy DiPaolo

Campus Address
231 S. Atherton Street, Apt. 4
State College, PA 16801

thd5025@gmail.com
Cell: (610) 955-8262
Home: (610) 989-9779

Permanent Address
1178 Rossiter Lane
Wayne, PA 19087

EDUCATION

The Pennsylvania State University University Park, PA Graduation: May 2015
Schreyer Honors College
Bachelor of Science in Chemical Engineering
Minor in Architecture Studies

RELATED WORK EXPERIENCE

Chemical Engineering University Park, PA May 2013 – Present
Undergraduate Research Assistant
- Analyze micelle formation using computerized molecular dynamics simulations
- Perform weekly presentations on findings
- Work with graduate students and faculty

Chart Energy & Chemicals, Inc. The Woodlands, TX May 2014 – August 2014
Process Engineering Intern
- Performed multiple dynamic simulation tests on liquefied natural gas plant
- Created bid tab for prospective suppliers
- Updated P&IDs and PFDs for various projects

OTHER WORK EXPERIENCE

The Learning Factory University Park, PA Aug 2013 – Present
Teaching Assistant
- Teach courses on proper equipment use for 15 student class
- Monitor shop and aid students working on machinery
- Meet with other Teaching Assistants biweekly to effectively oversee facility as a team

Student Painters Wayne, PA May – Aug 2012
Painter, Assistant Manager
- Made executive decisions and led a five-person team
- Performed exterior and interior house painting on 21 houses
- Developed interpersonal skills through discussions with clients

Kimmel Bogrette Architecture + Site Conshohocken, PA May – June 2011
Intern
- Visited the work sites of current projects
- Attended meetings with clients and employees
- Corrected project drawings using AutoCAD

SPECIAL SKILLS

DYNSIM, Gromacs, Mathematica, UNIX, LaTex, AutoCAD
Revit, Rhino, SketchUp, Adobe Suite, Microsoft Office Suite

HONORS

Dean's List Fall 2011 to Present
National Society of Collegiate Scholars Member
McWhirter Undergraduate Scholarship in Chemical Engineering Recipient 2014
Richard H. and Kay W. Klinger Scholarship in Chemical Engineering Recipient 2013
1st Place Charles Thorp Design Competition

LEADERSHIP & ACTIVITIES

American Institute of Chemical Engineers (AIChE) Member Aug 2013 – Present
Penn State Dance Marathon (THON) Committee Member …… Oct 2012 – May 2015
- Operations Committee Member (2012-14) and Hospitality Committee Member (2014-15)
- Fundraising Coordinator 2013-2015, Four Diamonds Recycling Effort Chair 2012- 2013
- Supports pediatric cancer research as the largest student-run philanthropy in the world

Penn State Track and Field Club Sept 2011 – Present
Wayne United Methodist Church Service Team Aug 2006 – Present
- Youth Leader Aug 2009 – Aug 2011
- Travel around the country providing construction labor for those in need